Nucleon and triton production from nucleon-induced reactions on ^{7}Li

Yukinobu Watanabe[1,a], Hairui Guo[1,4], Kohei Nagaoka[1], Takuma Matsumoto[2], Kazuyuki Ogata[3], and Masanobu Yahiro[2]

[1]*Department of Advanced Energy Engineering Science, Kyushu University, Kasuga, Fukuoka 816-8580, Japan*
[2]*Department of Physics, Kyushu University, Fukuoka 812-8581, Japan*
[3]*Research Center for Nuclear Physics, Osaka University, Ibaraki, Osaka 567-0047, Japan*
[4]*Institute of Applied Physics and Computational Mathematics, Beijing, 100094, China*

Abstract. Nucleon (N) and triton production from nucleon-induced reactions on ^{7}Li at an incident energy of 14 MeV are analyzed by using three-body continuum discretized coupled channels method (CDCC), final state interaction (FSI) model, and sequential decay (SD) model. The CDCC is used to describe nucleon and triton production via breakup continuum channels, ^{7}Li(N,N′)^{7}Li*$\rightarrow t + \alpha$. Triton production from $p(n)$ + ^{7}Li $\rightarrow t$ + ^{5}Li(^{5}He) channel and nucleon production from sequential decay of the ground-state ^{5}Li(^{5}He) are calculated by the FSI model and the SD model, respectively. The calculated double differential cross sections for both nucleon and triton production are in good agreement with experimental ones except at relatively low nucleon emission energies.

1 Introduction

In fusion technology, lithium is an important element for tritium breeding in D-T fusion reactors [1] as well as a candidate material for neutron converter in the intense neutron source of International Fusion Materials Irradiation Facility (IFMIF) [2]. From the point of view of the safety in IFMIF, it is also important to predict tritium production from nuclear reactions between lithium and nucleon emitted via deuteron stripping reaction. Regardless of the great significance of nucleon induced reactions on lithium, the experimental data are not necessarily sufficient. Therefore, theoretical study of these nuclear reactions is needed to provide accurate and reliable nuclear data, especially double differential cross sections (DDXs) of nucleon and triton production from ^{7}Li.

Since ^{7}Li is a weakly bound nucleus which can easily break up into two fragments, namely, ^{7}Li $\rightarrow t + \alpha$, the breakup channels are expected to be important reaction channels in nucleon induced reactions on ^{7}Li [3]. Thus, understanding of the breakup channels is essential to analyses of N + ^{7}Li reactions. However, conventional theoretical models such as DWBA method and statistical models cannot describe them well, because the breakup channels have to be described in the three-body system consisting of N, α and t, the breakup states of ^{7}Li are in continuum, and the breakup channel has

[a]e-mail: watanabe@aees.kyushu-u.ac.jp

a strong coupling with the elastic scattering channel, Therefore, systematic study of the ^{7}Li breakup mechanism is an interesting and meaningful subject not only in fusion applications, but also in nuclear physics itself.

Recently, Ichinkhorloo *et al.* [4] have applied three-body continuum discretized coupled channels method (CDCC)[5, 6] with the JLM N-N interaction [7] to n +^{7}Li scattering for incident energies below 24 MeV. Their result reproduces well experimental angular distributions for neutron elastic and inelastic scattering from ^{7}Li and double differential (n, xn) cross sections at relatively high emission energies for incident energies between 11.5 and 24.0 MeV. However, they did not analyze triton production from the breakup process of ^{7}Li.

In our early work [3], both neutron and proton scatterings from ^{7}Li were analyzed over a wide incident energy range up to 150 MeV using three-body CDCC with the JLM N-N interaction considering only P and F internal states of ^{7}Li. The energy dependence of the normalization factors of the JLM N-N interaction was investigated and its empirical expression was obtained from the analysis. The CDCC calculation reproduced the experimental data of neutron total, proton reaction cross sections, and elastic and inelastic scattering angular distributions well. The importance of the breakup effect was demonstrated by analyzing the effect of the coupling between breakup and elastic channels on differential elastic scattering cross section. However, we did not analyze simultaneously nucleon and triton production processes via the breakup channels.

In the present work, we calculate DDXs for nucleon and triton production from the following two reaction processes:

$$p(n) + ^7\mathrm{Li} \rightarrow p'(n') + ^7\mathrm{Li}^* \rightarrow p'(n') + \alpha + t, \qquad (a)$$

$$p(n) + ^7\mathrm{Li} \rightarrow t + ^5\mathrm{Li}(^5\mathrm{He}) \rightarrow t + p'(n') + \alpha, \qquad (b)$$

where ^{7}Li* denotes the ^{7}Li in the breakup continuum states excited by nucleon inelastic scattering. Both nucleon and triton emissions via the breakup channel (a) in proton and neutron induced reactions at 14 MeV are analyzed using the full CDCC. The nucleon and triton production DDXs from the breakup channel are obtained consistently, which is a more straightforward way to demonstrate the applicability of CDCC to the analysis of the breakup channels of nucleon induced reactions on ^{7}Li. In addition, the triton and nucleon emissions from the reaction process (b) are also calculated by a final state interaction (FSI) model[8] and a sequential decay (SD) model[9], respectively.

Section 2 describes a method of calculating nucleon and triton production DDXs in terms of CDCC, FSI model, and SD model. In Sect. 3, calculated results are compared with experimental data and discussed. Finally, Section 4 gives a summary and conclusion.

2 Theoretical Model

Nucleon and triton production processes from the breakup channel (a) and the reaction channel (b) of nucleon induced reactions on ^{7}Li are analyzed by using the following hybrid approach consisting of CDCC, FSI, and SD models.

2.1 CDCC for analysis of the breakup channel

CDCC is an extension of coupled channels methods, in which the breakup continuum states of the weakly bound nucleus are truncated and discretized to the finite number of discrete states in terms of the relative linear and angular momentum of its fragments, and the discrete states are treated similarly to the usual bound inelastic states in the coupled channels method. The detailed formulation of CDCC for analyzing nucleon induced reactions on ^{7}Li is given in our previous paper [3]. The reactions are

analyzed using the N + t + α three-body model. The breakup continuum states of ^{7}Li are discretized by the pseudostate method [10, 11], and the diagonal and coupling potentials are obtained by folding the JLM effective N-N interaction with transition densities. In the work, the relative angular momentum l was truncated as $l \leq 3$, and even l states (S and D states) were ignored because their contributions are expected to be smaller than those of odd states. In the present work, the even states are considered as well.

Double differential (n, n') and (p, p') cross sections from the breakup channels (a) in the laboratory system are given by

$$\frac{d^2\sigma}{dE_{\rm N}^L d\Omega_{\rm N}^L} = \sum_{lI} \frac{1}{2I+1} \frac{\pi\mu_r}{\hbar^2 k P_0^2} \frac{m_{\rm N} + M_{\rm Li}}{M_{\rm Li}} \left(\frac{E_{\rm N}^L}{E_N^C}\right)^{1/2} \times \sum_{m_{I_0} m_I} \left| \sum_{L_0 LJ} \sqrt{2L+1} (I_0 m_{I_0} L_0 0 \mid J m_{I_0}) (I m_I L m_{I_0} - m_I \mid J m_{I_0}) Y_{L m_{I_0} - m_I}(\Omega_{\rm N}^C) S_{lIL}^J(k) \right|^2, \quad (1)$$

where $E_{\rm N}^L$ and $\Omega_{\rm N}^L$ are the energy and emission direction of the emitted nucleon in the laboratory system, and $E_{\rm N}^C$ and $\Omega_{\rm N}^C$ are those in the center-of-mass system. $m_{\rm N}$ and $M_{\rm Li}$ are the masses of incident nucleon and ^{7}Li, respectively. μ_r and $\hbar k$ are the reduced mass and relative momentum of the $t - \alpha$ system, respectively. $\hbar P_0$ is the incident momentum. l, I and m are the orbital angular momentum, the total spin and its projection on the z axis in the t-α system of ^{7}Li, respectively. L and J are the orbital and total angular momenta in the N - ^{7}Li system. The subscript 0 means the ground state of ^{7}Li. $S_{lIL}^J(k)$ is the S-matrix element.

According to Refs. [13–15], the triple differential cross section of the breakup fragments in the laboratory system is expressed as

$$\frac{d^3\sigma}{d\Omega_t dE_t d\Omega_\alpha} = \frac{2\pi}{\hbar} \frac{\mu}{P_0} \left|T_{fi}\right|^2 \rho(E_t), \quad (2)$$

where Ω_t and Ω_α represent the emission direction of t and α, respectively. E_t is the emission energy of t and μ is the reduced mass of the N - ^{7}Li system. $\rho(E_t)$ is the phase space factor [13, 14, 16] expressed as

$$\rho(E_t) = \frac{m_t m_\alpha m_{\rm N} P_t P_\alpha}{(2\pi\hbar)^6 \left[m_\alpha + m_{\rm N} + \dfrac{m_\alpha (\boldsymbol{P}_t - \boldsymbol{P}_{tot}) \cdot \boldsymbol{P}_\alpha}{P_\alpha^2} \right]}, \quad (3)$$

where m_t and m_α are the masses of t and α, respectively. $\hbar\boldsymbol{P}_t$ and $\hbar\boldsymbol{P}_\alpha$ are the momenta of the emitted t and α, respectively. $\boldsymbol{P}_{tot}$ is the total momentum of the three-body system. The transition matrix element, T_{fi}, is given by [13, 15]

$$T_{fi} = i \frac{(2\pi\hbar)^3}{\sqrt{2\mu\mu_r}} \frac{1}{k\sqrt{PP_0}} \sum_{lILJM} \sqrt{2J+1} [Y_l(\hat{\boldsymbol{k}}) \otimes Y_L(\hat{\boldsymbol{P}})]_{JM} e^{i(\delta_{lIk} + \sigma_{lIk})} S_{lIL}^J(k), \quad (4)$$

where $\hbar\boldsymbol{P}$ is the momentum of N relative to ^{7}Li. $\hat{\boldsymbol{k}}$ and $\hat{\boldsymbol{P}}$ are the direction of $\hbar\boldsymbol{k}$ and $\hbar\boldsymbol{P}$, respectively. δ_{lIk} and σ_{lIk} are the nuclear and Coulomb phase shifts between t and α, respectively.

The triton production DDX from the breakup channel (a) is then obtained by

$$\frac{d^2\sigma}{d\Omega_t dE_t} = \int d\Omega_\alpha \frac{d^3\sigma}{d\Omega_t dE_t d\Omega_\alpha}. \quad (5)$$

2.2 Final state interaction model

The FSI model [8] is used for the calculation of triton production from the reaction channel (*b*). ^{5}He and ^{5}Li are considered as α - n and α - p systems, respectively. The formula is expressed as

$$\left(\frac{d^2\sigma}{d\Omega_t dE_t}\right)_{\rm FSI} = N_F \sin^2\beta_l \frac{F_l^2(k_{{\rm N}\alpha}a) + G_l^2(k_{{\rm N}\alpha}a)}{(k_{{\rm N}\alpha}a)^2}\rho(E_t), \tag{6}$$

where N_F is the normalization factor determined by fitting to experimental data, F_l and G_l are the first-order spherical Bessel functions for the α - n system and the Coulomb wave functions for the α - p system, k denotes the wave number of $p(n)$ in α - $p(n)$ system, a denotes the channel radius, and ρ is the phase space factor. β_l means for the α - $p(n)$ phase shift, which is calculated by

$$\beta_l = \tan^{-1}[\frac{1}{2}\Gamma_\lambda/(E_\lambda + \Delta_\lambda - E_{{\rm N}\alpha})], \tag{7}$$

with

$$\Delta_\lambda = \frac{1}{2}\Gamma_\lambda(F_l F_l' + G_l G_l'), \tag{8}$$

$$\frac{1}{2}\Gamma_\lambda = \frac{\gamma^2 k_{{\rm N}\alpha}a}{(F_l^2 + G_l^2)}. \tag{9}$$

The parameters necessary to obtain β_l are taken from Ref. [17] for the α - p system and Ref. [18] for the α - n system: $E_\lambda = -3.3$ MeV, $a = 3.0$ fm and $\gamma^2 = 8.23$ MeV for ^{5}Li, and $E_\lambda = -4.93$ MeV, $a = 3.0$ fm and $\gamma^2 = 7.89$ MeV for ^{5}He.

2.3 Sequential decay model

Nucleon emission DDXs from the decay of ground-state ^{5}Li(^{5}He) in the reaction channel (*b*) can be calculated with the SD model [9]. The formula is expressed as

$$\frac{d^2\sigma}{d\Omega_{\rm N'}dE_{\rm N'}} = \frac{\sigma_t^{FSI}}{2\pi}\int L_1(E_{\rm N} \rightarrow E_{^5{\rm Li}(^5{\rm He})})L_2(E_{^5{\rm Li}(^5{\rm He})} \rightarrow E_{\rm N'})\Lambda(\eta_{\rm NN'})dE_{^5{\rm Li}(^5{\rm He})}, \tag{10}$$

where σ_t^{FSI} is the triton production cross section obtained with FSI model. L_1 denotes the probability that an incident nucleon with energy $E_{\rm N}$ produces an intermediate ^{5}Li(^{5}He) with energy $E_{^5{\rm Li}(^5{\rm He})}$. L_2 denotes the probability that the intermediate ^{5}Li(^{5}He) with energy $E_{^5{\rm Li}(^5{\rm He})}$ produces a nucleon with energy $E_{\rm N'}$. $\Lambda(\eta_{\rm NN'})$ means the probability of the cosine of the angle between the direction of incident nucleon and emitted nucleon being $\eta_{\rm NN'}$. L_1 and L_2 are expressed as

$$L_1 = \pi\Theta_1(m_{\rm N} + M_{\rm Li})\left[\frac{m_{\rm N}m_t M_{^5{\rm Li}(^5{\rm He})}}{m_t + M_{^5{\rm Li}(^5{\rm He})}}E_{\rm N}\left(\frac{M_{\rm Li}}{m_{\rm N} + M_{\rm Li}}E_{\rm N} + Q_1\right)\right]^{-1/2}, \tag{11}$$

$$L_2 = \pi\Theta_2\left[\frac{m_{\rm N}m_\alpha E_{^5{\rm Li}(^5{\rm He})}Q_2}{M_{^5{\rm Li}(^5{\rm He})}(m_{\rm N} + m_\alpha)}\right]^{-1/2}, \tag{12}$$

where Q_1 and Q_2 are the reaction Q values for ^{5}Li(^{5}He) production and ^{5}Li(^{5}He) decay, respectively. Θ_1 is the angular distribution of the intermediate ^{5}Li(^{5}He) which is obtained from the triton production DDX calculated with FSI. The nucleon emission is assumed to be isotropic, then the angular distribution of the nucleon emission in the N-α system is expressed as

$$\Theta_2 = \frac{1}{4\pi}. \tag{13}$$

3 Results and discussion

3.1 Proton induced reaction on ^{7}Li at 14 MeV

The proton and triton emission DDXs from the breakup channel (*a*) in proton induced reactions on ^{7}Li are calculated within the framework of CDCC. Fig. 1 shows comparisons of the CDCC result and the experimental data [19] of inclusive proton emission DDXs at an incident energy of 14 MeV. The experimental proton emission data contain the influence of contamination in the target, such as hydrogen(H), carbon(C), and oxygen(O), which is denoted in the figures. The contributions corresponding to unbound $^{3/2}$P, $^{1/2}$P, $^{1/2}$S, $^{3/2}$D, $^{5/2}$D, $^{7/2}$F and $^{5/2}$F states of ^{7}Li are denoted by dashed, dotted, dash-dotted, dash-dot-dotted, short-dashed, short-dotted and short-dash-dotted lines, respectively. The total CDCC result including (*p*,*p*') scattering from the bound states of ^{7}Li is shown by the thick solid lines. Four peaks seen in the total CDCC result represent the elastic, inelastic scattering to the first excited state, $7/2^{-}$ and $5/2^{-}$ resonance states, respectively, from the high emission energy end. The CDCC calculation reproduces the experimental data reasonably well in the relatively high emission energy region, whereas the calculated results underestimate the experimental data at low emission energies remarkably. The underestimation is caused by neglecting the other reaction channels including the reaction channel (*b*) which cannot be calculated with the present CDCC as discussed later.

The CDCC result of the triton production DDX from the breakup channel (*a*) at 14 MeV is shown by the thick solid lines in Fig. 2. The calculated results overestimate slightly the experimental data [20] at low emission energies. It may be due to overestimation of the contribution from the unbound $^{3/2}$P state of ^{7}Li. In addition, the calculated results underestimate considerably the experimental data at relatively high emission energies. The discrepancy at high emission energies is due to the contribution from the reaction channel (*b*), as mentioned later.

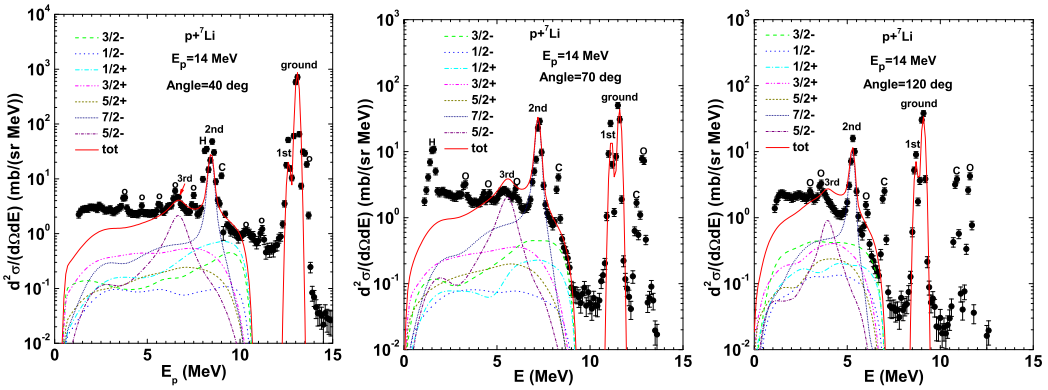

Figure 1. CDCC result of the proton emission DDX for p + ^{7}Li reaction at 14 MeV compared with the experimental data [19]. The dashed, dotted, dash-dotted, dash-dot-dotted, short-dashed, short-dotted and short-dash-dotted lines denote the contributions corresponding to unbound $^{3/2}$P, $^{1/2}$P, $^{1/2}$S, $^{3/2}$D, $^{5/2}$D, $^{7/2}$F and $^{5/2}$F states of ^{7}Li, respectively.

Since it is expected that the discrepancy between the CDCC calculations and experimental DDXs seen in Figs. 1 and 2 is due to neglecting the contribution from the reaction channel (*b*), the triton production DDXs from the reaction channel (*b*) are predicted by the FSI model, and the nucleon emission from the sequential decay of the intermediate ^{5}Li(^{5}He) in (*b*) is calculated with the SD model. In Fig. 3, the triton production DDXs calculated with the FSI model are shown by the dashed

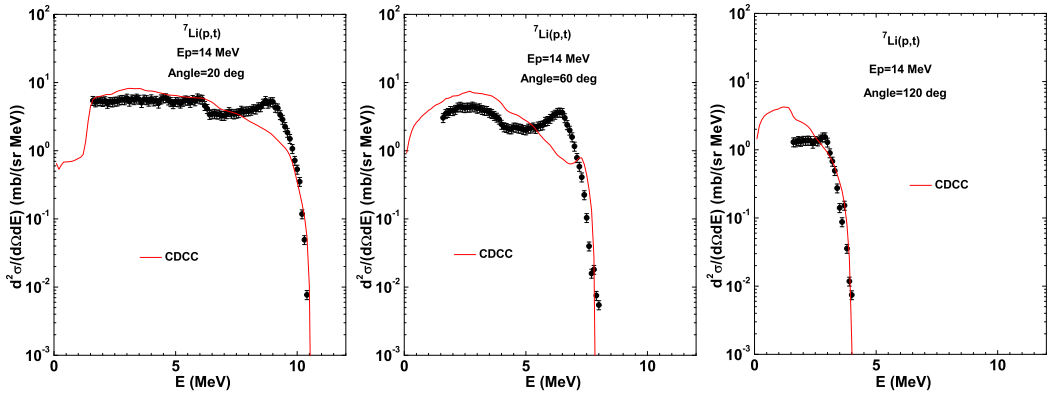

Figure 2. Comparison of triton production DDXs calculated by CDCC with experimental data for p + ^{7}Li reaction at 14 MeV [20].

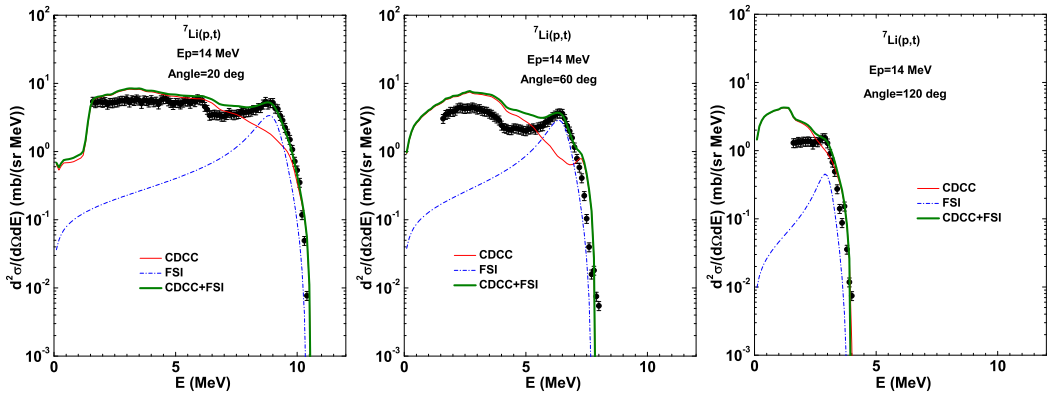

Figure 3. The calculated triton production DDX compared with experimental data for p + ^{7}Li reaction at 14 MeV. The explanation of each line is given in the text.

lines. The normalization factor N_F in Eq. (6) for each angle is determined so as to reproduce the experimental broad peak seen in the high emission energy region. The summation of FSI and CDCC calculations reproduce the experimental data reasonably well over a wide range of triton emission energy, although the calculation overestimates slightly the experimental data in the low emission energy region. On the other hand, the proton emission from the reaction channel (b) for the p + ^{7}Li reaction at 14 MeV shown by the dashed lines in Fig. 4 contributes mainly to the low emission energy region. The summation of the contribution from the reaction channel (b) and the CDCC result is shown by the thick solid lines. The result improves the agreement with the experimental data considerably well. For the proton emission DDX, however, it still underestimates the experimental data for small angles in the low emission energy region because of the other reaction processes contributing to this energy region still exist, such as (p, np) and $(p, 2p)$ reactions.

Figure 5 shows the calculated angular distribution of 14 MeV (p, t) reaction on ^{7}Li. The dashed line denotes the component calculated by the FSI model, where the cross section at 0° is assumed

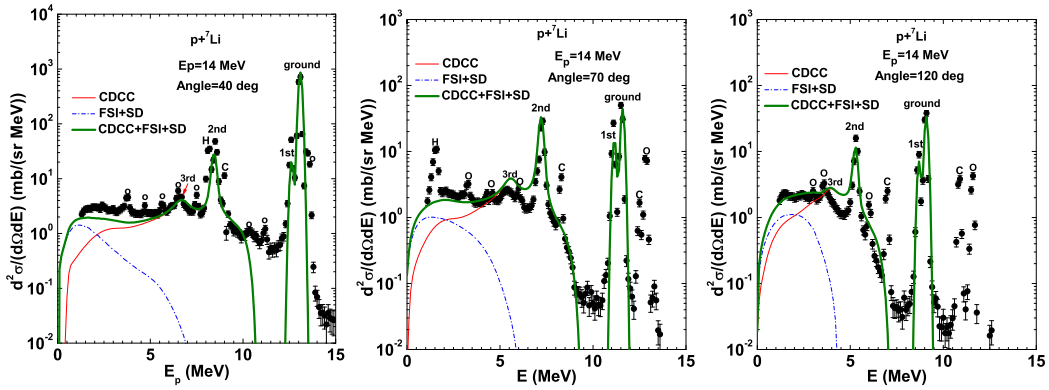

Figure 4. The calculated proton emission DDX from both reaction channels (*a*) and (*b*) compared with experimental data for p + ^{7}Li reaction at 14 MeV. The explanation of each line is given in the text.

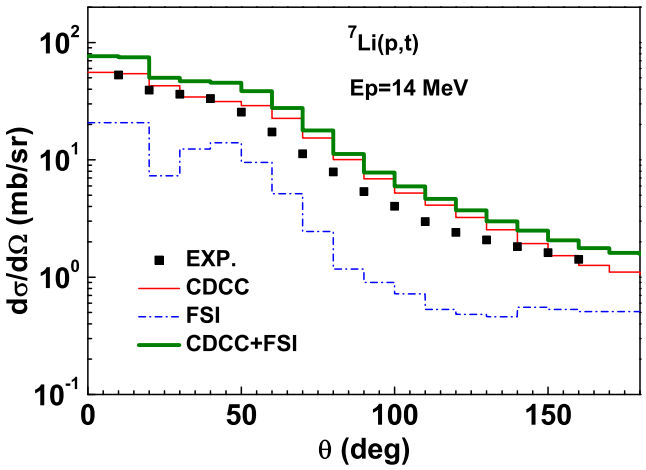

Figure 5. Comparison of the angular distribution of the ^{7}Li (p,t) reaction at 14 MeV with the experimental data (solid circles). The thin solid line, the dashed line and the thick solid line denote the CDCC result, the FSI result and the summation of CDCC and FSI results, respectively.

to be the same as that at 10° because of no experimental data. The thick solid line represents the summation of the CDCC component (thin solid line) and the FSI one, the shape of which is consistent with the experimental data [20], although the magnitude is a little larger.

3.2 Neutron induced reaction on ^{7}Li at 14 MeV

The neutron emission DDXs from the breakup channel (*a*) in neutron induced reactions on ^{7}Li are calculated with CDCC. In Fig. 6, comparisons of the CDCC results and the experimental data [21] of the inclusive neutron emission DDXs are shown at an incident energy of 14.2 MeV. The first peak of the experimental data from high emission energy end denotes the summation of elastic and first

inelastic scattering components because of the poor energy resolution, and the second and third peaks correspond to the inelastic scattering to the $7/2^-$ and $5/2^-$ resonance states, respectively. The CDCC calculation results are in good agreement with the experimental data in the relatively high neutron emission energy region, while the calculated results underestimate the experimental data in the low emission energy region. As shown later in Fig. 7, the underestimation is due to the other missing reaction channels, such as the reaction channel (*b*), which cannot be calculated within the framework of the present CDCC.

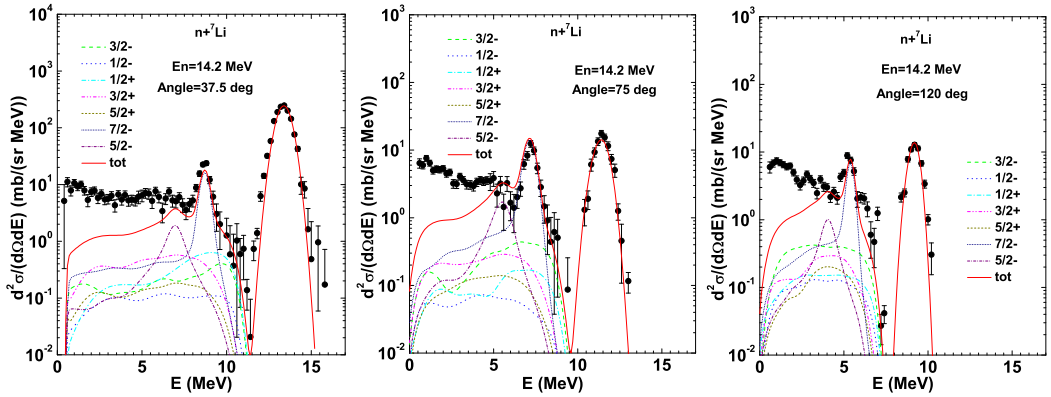

Figure 6. CDCC result (solid lines) of the neutron emission DDX for n + ^{7}Li reaction at 14.2 MeV compared with the experimental data[21]. The dashed, dotted, dash-dotted, dash-dot-dotted, short-dashed, short-dotted and short-dash-dotted lines denote the contributions corresponding to unbound $^{3/2}$P, $^{1/2}$P, $^{1/2}$S, $^{3/2}$D, $^{5/2}$D, $^{7/2}$F and $^{5/2}$F states of ^{7}Li, respectively.

Next, DDXs of inclusive neutron and triton emissions from both the reaction channels (*a*) and (*b*) at incident energies of 14.2 and 14 MeV are calculated by using the hybrid approach of CDCC+FSI+SD, and shown in Figs. 7 and 8, respectively. The FSI calculation for the reaction channel (*b*) requires the experimental data of triton production DDXs. However, only the experimental data [22] are available for the emission angle of 0° at 14 MeV. We assume that the shape of (n, t) angular distributions for the reaction channel (*b*) is same as that of the (p, t) ones given in Fig. 5. Then, the FSI result of the (n, t) angular distribution is obtained by normalizing that of the (p, t) angular distribution at 0°. From Figs. 7 and 8, it can be seen that neutron and triton production from the reaction channel (b) contributes mainly to the low neutron and high triton emission energy regions. The summation of both the contributions from the reaction channels (a) and (b) is denoted by the thick solid line. The summation results are in good agreement with the experimental data [21, 22] except for the neutron emission DDXs in the low emission energy region where it is expected that the other reaction processes contributing to this energy region still exist, such as (n, $2n$) reaction.

4 Summary and conclusion

The nucleon and triton production processes in nucleon induced reactions on ^{7}Li at 14 MeV are analyzed by using the three-body CDCC, final state the interaction (FSI) model, and the sequential decay (SD) model. The double differential cross sections (DDXs) for nucleon and triton production from the reaction process via breakup channels of ^{7}Li,

$$p(n) + {}^7\mathrm{Li} \rightarrow p'(n') + {}^7\mathrm{Li}^* \rightarrow p'(n') + \alpha + t,$$

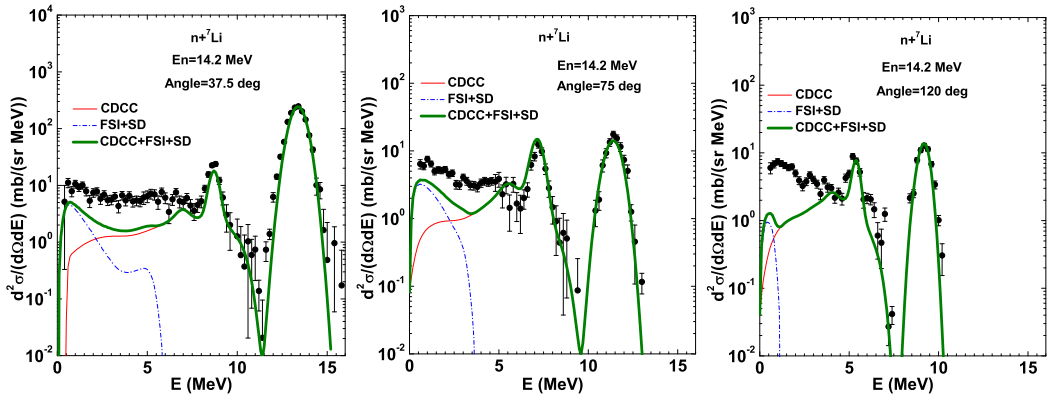

Figure 7. Same as Fig. 4 but for the n + ^{7}Li reaction at 14.2 MeV.

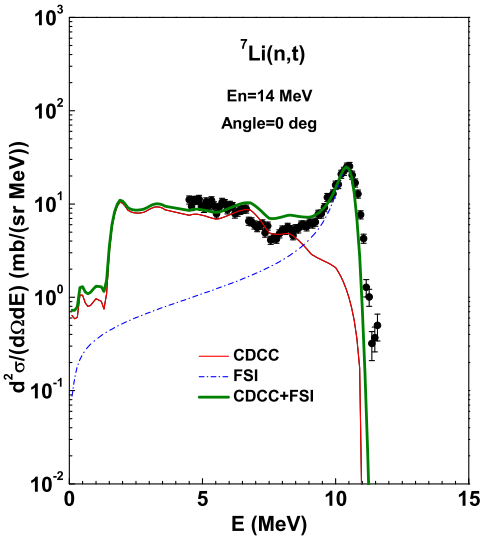

Figure 8. Same as Fig. 3 but for the n + ^{7}Li reaction at 14 MeV.

are calculated using the CDCC. The calculated result for nucleon emission reproduces the experimental DDXs fairly well at relatively high emission energies. The CDCC results of triton production DDXs overestimate slightly the experimental data at low triton emission energies. This may be because the contribution from the unbound $^{3/2}$P state of ^{7}Li is overestimated.

Next, the triton and nucleon emission DDXs from the reaction channel,

$$p(n) + {}^{7}\mathrm{Li} \rightarrow t + {}^{5}\mathrm{Li}({}^{5}\mathrm{He}) \rightarrow t + p'(n') + \alpha,$$

are calculated with the FSI and SD models, respectively. The result supplements the remarkable underestimation seen in the CDCC results at high triton emission energies and low nucleon emission energies.

Through the present analysis, it has been clarified that the breakup continuum channels play an essential role in triton production from nucleon induced reactions on ^{7}Li at 14 MeV. Since the present FSI model needs the experimental triton emission DDXs to determine the magnitude of cross sections, a theoretical model which can describe transfer or knock-on (p,t) reaction leading to three body final states will be required for further study of the incident energy dependence of the FSI component. In addition, a statistical decay model calculation will be necessary to compensate the underestimation seen in the low nucleon emission energy region by considering nucleon emissions from highly excited states of ^{7}Li*, such as (n,2n) or (p,2p) reactions.

Acknowledgments

We would like to thank Satoshi Chiba for helpful discussion and comments. We are also grateful to Norihiko Koori for providing the experimental data of ^{7}Li(p, xp) and (p, xt) reactions at 14 MeV and useful comments on the measurement. This work was supported by Grant-in-Aid for Scientific Research of the Japan Society for the Promotion of Science (No. 22560820).

References

[1] ITER - the way to new energy, http://www.iter.org.
[2] P. Garin, M. Sugimoto, J. Nucl. Mater. **417**, 1262 (2011), and references therein.
[3] H. Guo, Y. Watanabe, T. Matsumoto, K. Ogata, M. Yahiro, Phys. Rev. C **87**, 024610 (2013).
[4] D. Ichinkhorloo, Y. Hirabayashi, K. Katō, M. Aikawa, T. Matsumoto, S. Chiba, Phys. Rev. C **86**, 064604 (2012).
[5] M. Kamimura, M. Yahiro, Y. Iseri, Y. Sakuragi, H. Kameyama, M. Kawai, Prog. Theor. Phys. Suppl. **89**, 1 (1986).
[6] M. Yahiro, K. Ogata, T. Matsumoto, K. Minomo, Prog. Theor. Exp. Phys. **2012**, 01A206 (2012), and references therein.
[7] J.P. Jeukenne, A. Lejeune, C. Mahaux, Phys. Rev. C **16**, 80 (1977).
[8] T. Rausch, H. Zell, D. Wallenwein, W-Von. Witsch, Nucl. Phys. A **222**, 429 (1974).
[9] T. Beynon, B. Sim, Ann. Nucl. Energy **15**, 27 (1988).
[10] A.M. Moro, J.M. Arias, J. Gomez-Camacho, I. Martel, F. Perez-Bernal, R. Crespo, F. Nunes, Phys. Rev. C **65**, 011602 (2001).
[11] T. Matsumoto, T. Kamizato, K. Ogata, Y. Iseri, E. Hiyama, M. Kamimura, M. Yahiro, Phys. Rev. C **68**, 064607 (2003).
[12] R.J. Spiger, and T.A. Tombrello, Phys. Rev. **163**, 964 (1967).
[13] Y. Iseri, M. Yahiro, M. Kamimura, Prog. Theor. Phys. Suppl. **89**, 84 (1986).
[14] G.G. Ohlsen, Nucl. Instr. Meth. **37**, 240 (1965).
[15] M. Yahiro, Y. Iseri, M. Kamimura, M. Nakano, Phys. Lett. B **141**, 19 (1984).
[16] H. Fuchs, Nucl. Instr. Meth. **200**, 361 (1982).
[17] A. Barnard, C. Jones, J. Weil, Nucl. Phys. **50**, 604 (1964).
[18] G.L. Morgan, R.L. Walter, Phys. Rev. **168**, 1114 (1968).
[19] N. Koori, I. Kumabe, M. Hyakutake, K. Orito, K. Akagi, A. ida, Y. Watanabe, K. Sagara, H. Nakamura, K. Maeda, T. Nakashima, M. Kamimura, Y. Sakuragi, JEARI-M 89-167 (1989).
[20] N. Koori, I. Kumabe, M. Hyakutake, Y. Watanabe, K. Orito, K. Akagi, A. Iida, M. Eriguchi, Y. Wakuta, K. Sagara, H. Nakamura, K. Maeda, T. Nakashima, JEARI-M 91-009 (1991).

[21] S. Chiba, M. Baba, H. Nakashima, M. Ono, N. Yabuta, S. Yukinori, N. Hirakawa, J. Nucl. Sci. Technol. **22**, 771 (1985).
[22] V. Valković, Nucl. Phys. **60**, 581 (1964).